ELSEVIER

Thermochimica Acta 379 (2001) 131–145

thermochimica acta

www.elsevier.com/locate/tca

Calorimetric and spectroscopic study of the coordinative unsaturation of copper(I) and silver(I) cations in ZSM-5 zeolite Room temperature adsorption of NH_3

Vera Bolis[a,*], Silvia Bordiga[b], Gemma Turnes Palomino[b], Adriano Zecchina[b], Carlo Lamberti[b,c]

[a]*DiSCAFF, Università del Piemonte Orientale "A. Avogadro", viale Ferrucci 33, 28100 Novara, Italy*
[b]*Dipartimento di Chimica IFM, Università di Torino, via P. Giuria 7, 10125 Torino, Italy*
[c]*Unità INFM, Università di Torino, via P. Giuria 7, 10125 Torino, Italy*

Abstract

The room temperature (RT) adsorption of NH_3 was used to probe the coordinative unsaturation of Cu(I) and Ag(I) cations highly dispersed in ZSM-5 zeolites. Adsorption microcalorimetry allowed to characterise both quantitatively and energetically the amino complexes formed at the cationic sites, as revealed by IR spectroscopy. Copper(I) sites were found to form tetra-amino $[Cu(NH_3)_4]^+$ adducts, whereas silver(I) ones do form only di-amino $[Ag(NH_3)_2]^+$ species. Both results are in agreement with the homogeneous chemistry of Cu(I) and Ag(I) cations. The heat of formation of the different amino-complexes was found to be comprised in the 130–50 kJ/mol interval for both kind of Me(I) sites, according to the number of ligands progressively bound and in spite of the different stoichiometry of the species formed. The adducts were found to be only partially reversible upon outgassing in the adopted conditions (303 K and $p \approx 10^{-5}$ Torr). Two distinct, nearly equally populated families of sites were revealed in both Me(I)-ZSM-5 samples, corresponding to different coordinative unsaturations of the metal cations. EXAFS data, used to check the local environment of noble metal cations, confirmed the proposed model. In the case of Cu(I) sites, the formation of mixed amino-carbonyl complexes was also studied. The thermodynamic stability of amino- and carbonyl-like species was found not to be the same.

Keywords: Adsorption enthalpy; Microcalorimetry; Ammonia; Copper(I); Silver(I); EXAFS spectroscopy; IR spectroscopy; Zeolites; Catalysis

1. Introduction

Noble metal-exchanged zeolites are active catalysts in economically important processes. In particular, Cu(I)-ZSM-5 zeolite is of greatest interest for the direct conversion of NO into N_2 and O_2 [1–3] while Ag(I)-ZSM-5 shows high activity in several catalytic and photocatalytic processes [4]. Among them the most important is the photochemical dissociation of H_2O in H_2 and O_2 [5,6]. In both copper [7–9] and silver [10–12] cases, the metal-exchanged zeolites are much more active than the other supported noble metal based catalysts, suggesting that the unique catalytic properties of these systems are probably

* Corresponding author. Tel.: +39-321-657-613; fax: +39-321-657-621.
E-mail address: bolis@pharm.unipmn.it (V. Bolis).

0040-6031/01/$ – see front matter
PII: S0040-6031(01)00612-8

related to the high coordinative unsaturation of the extra-framework cations hosted in the MFI structure.

Beside their interest as catalytic systems, zeolites are also of greatest interest in that their three-dimensionally organised porous structure allows stable species like small metal clusters and coordination complexes [13–17] to form in the zeolite cavities. Cu(I) cations highly dispersed in the zeolite framework are able to form at room temperature (RT) relatively stable adducts such as the "end-on" $[Cu(N_2)]^+$ species [8,18] as well as mono-carbonyl $[Cu(CO)]^+$ and di-carbonyl $[Cu(CO)_2]^+$ complexes [8,19]. These species evolve to tri-carbonyl $[Cu(CO)_3]^+$ complexes at low temperature (≈100 K) [8,19,20]. In contrast, the extra-framework Ag(I) cations do not form at all adducts at RT with N_2, $[Ag(N_2)]^+$ complexes being observed only at $T \approx 100$ K [21], and the only carbonyl-like species they form are the mono-carbonyl $[Ag(CO)]^+$ ones, that evolve to the di-carbonyl $[Ag(CO)_2]^+$ species only at low temperature [22]. These data suggest that the adducts the two cations do form are characterised by a lower coordination number for Ag(I) with respect to Cu(I), in agreement with the homogeneous chemistry behaviour: the typical coordination number for Cu(I) is four (tetrahedral geometry) whereas is two for Ag(I) (linear geometry) [23]. The two group-11 Cu(I) and Ag(I) cations have indeed electronic similarities ($3d^{10}$ and $4d^{10}$ valence shell electronic configuration, respectively) but different size (rCu(I) = 0.96 Å and rAg(I) = 1.26 Å).

The complexity of the interaction between transition-metal-exchanged zeolites and reactants molecules in the catalytic processes of interest is not well understood yet, and this hinders a deep understanding of the processes. The aim of the present work is to investigate the RT interaction of NH_3 with coordinatively unsaturated Cu(I) and Ag(I) cations highly dispersed in ZSM-5 zeolites. The energetics of the formation of the amino-complexes, their stoichiometry and their stability upon outgassing was investigated by adsorption microcalorimetry. In the case of Cu(I)-ZSM-5, the formation of mixed amino-carbonyl species at the metallic sites was also studied. The nature of the species formed in the zeolite cavities was monitored by FT-IR spectroscopy. EXAFS data allowed to check the local environment of noble metal cations in the zeolite cavities as well as to determine structural parameters needed for a better comprehension of the species formed in the adsorption processes under study [24].

2. Experimental

2.1. Materials

2.1.1. Cu(I)-ZSM-5 and Ag(I)-ZSM-5

The noble metals exchanged zeolites were prepared starting from the same NH_4-ZSM-5 precursor (Si/Al = 14, EniChem SpA, Centro Ricerche di Novara). The exchange procedure was done in two steps. First, a thermal treatment in vacuo ($p \leq 10^{-3}$ Torr; 1 Torr = 133.3 Pa; 673 K, 6 h) caused the ammonium ions to decompose giving rise to the H-ZSM-5 protonic form of the zeolite. In the second step, the acidic proton was exchanged with the monovalent noble metal cation, but different exchange procedures were followed for the two samples. In the case of Cu(I)-ZSM-5, in order to obtain a model solid containing the sole copper(I) cations, the conventional procedure employing aqueous solution of copper(II) salts and subsequent reduction of Cu(II) to Cu(I) cations [25] could not be applied. Copper(I) ions were indeed directly introduced in the zeolite by using a non-conventional gas phase exchange employing CuCl, as described in details elsewhere [19]. Care was taken not to expose the Cu(I)-ZSM-5 so obtained to the air, in order to avoid the oxidation of Cu(I) to Cu(II) [26]. On the contrary, in the case of Ag(I)-ZSM-5, the conventional procedure employing an aqueous solution of $AgNO_3$ was applied. Care was taken to prevent, as much as possible, exposure of Ag(I)-ZSM-5 samples to light, since long exposures can lead to a partial photoreduction of Ag(I) cations and formation of metal clusters of the $[Ag_n]^{x+}$ type [21,22].

In both Cu(I)- and Ag(I)-ZSM-5 zeolites, a nearly total exchange was obtained (corresponding to one Cu(I) or Ag(I) cation for every framework Al atom) as evidenced by the IR spectra reported in Fig. 1. Indeed in the figure, where the IR spectra of the H-ZSM-5 (top side curve) and of Cu(I)- and Ag(I)-ZSM-5 (bottom side curves) samples are reported in the 3800–3500 cm^{-1} interval, the band of the O–H stretching of bridged Si–(OH)–Al groups located at ≈3610 cm^{-1} in the case of H-ZSM-5 is virtually

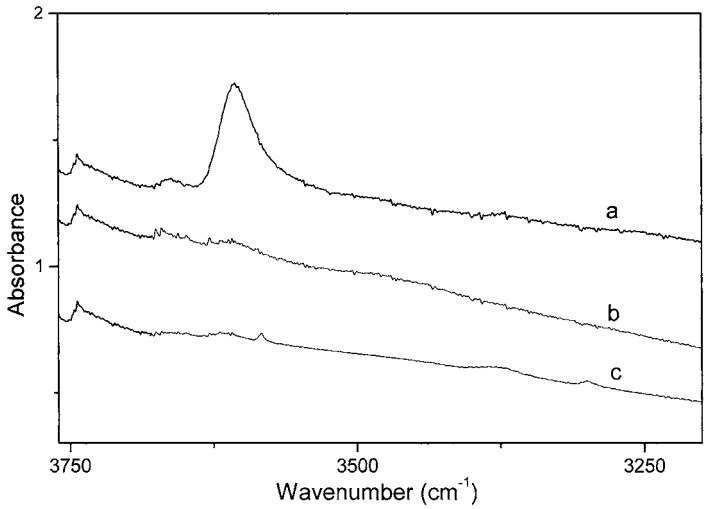

Fig. 1. IR spectra of the OH groups stretching region in the case of H-ZSM-5 (curve a), Cu(I)-ZSM-5 (curve b) and Ag(I)-ZSM-5 (curve c) zeolites. The H-ZSM-5 and Cu(I)-ZSM-5 samples were outgassed at 673 K, 2 h; the Ag(I)-ZSM-5 sample was outgassed at 400 K, 1 h.

totally absent in the spectra of Cu(I)- and Ag(I)-ZSM-5 samples. By contrast, the high frequency band at ≈3748 cm^{-1}, due to the OH stretching frequency of the zeolite SiOH groups was found to remain virtually unaffected by the exchange procedure.

2.2. Methods

2.2.1. Microcalorimetry

The heats of adsorption were measured at 303 K by means of a heat-flow microcalorimeter (Tian–Calvet type, Setaram, France) following a well-established stepwise procedure, previously described [27,28]. The calorimeter was connected to a high vacuum ($p \leq 10^{-5}$ Torr) gas-volumetric glass apparatus, that enabled to determine simultaneously the adsorbed amounts and the heats evolved for small increments of the adsorptive, up to an equilibrium pressure of 80–90 Torr. The pressure was monitored by means of a transducer gauge (Barocel 0–100 Torr, Edwards). A first run of adsorption was performed on the samples previously outgassed at the chosen activation temperature (673 K, 2 h for Cu(I)-ZSM-5 and 400 K, 1 h for Ag(I)-ZSM-5). Different activation conditions were followed in the two cases, because in the copper case we had to ensure the complete elimination of the CuCl cap protecting Cu(I) sites located in the channels of the zeolite [19,26] whereas in the silver(I) case milder activation conditions had to be chosen in order to obtain the desired degree of dehydration avoiding as much as possible photoreduction [21,22]. A second run was performed after outgassing (14 h, $p \leq 10^{-5}$ Torr) the sample at the calorimeter temperature, in order to evaluate the contribution of the reversible component to the adsorption. A third run was eventually performed after outgassing the sample at the same temperature but for a longer time (60 h, $p \leq 10^{-5}$ Torr) in order to check to what extent the amount of the reversible component does depend on the outgassing time.

2.2.2. Infrared spectroscopy

For IR measurements, thin self-supporting wafers of Cu(I)- and Ag(I)-ZSM-5 zeolites were prepared and activated by outgassing at the same temperature as for the volumetric-calorimetric experiments, under a dynamical vacuum of $p \approx 10^{-4}$ Torr, inside an IR cell specially designed to allow in situ high temperature treatments and gas dosage, as well as low-temperature measurements. The IR spectra were recorded at 2 cm^{-1} resolution on a BRUKER FT-IR 66 spectrometer equipped with an HgCdTe cryodetector.

2.2.3. EXAFS spectroscopy

Cu–K and Ag–K edge EXAFS spectra have been collected at the EXAFS1 station of LURE

(Orsay, France) and of the BM29 beamline at the European Synchrotron Radiation Facility (ESRF, Grenoble, France), respectively. In both cases, the angle/energy calibration was obtained by measuring the edge position of the corresponding metal foil. Each EXAFS spectrum, measured in transmission mode, was recorded three times under the same experimental conditions, and extracted $\chi(k)$ were averaged before the EXAFS data analysis. Standard deviation calculated from the averaged spectra was used to estimate the weight of statistical noise in the evaluation of the error associated with each structural parameters. The EXAFS data analysis was performed following standard procedures [29] and using Michalowicz's programs [30] as already described in [8,22].

3. Results and discussion

3.1. Local environment of Cu(I) and Ag(I) as determined by EXAFS

In Fig. 2, the k^3-weighted phase corrected Fourier transforms (FT) for both Cu(I)-ZSM-5 (full line) and Ag(I)-ZSM-5 (dotted line) are reported. In the case of Cu(I)-ZSM-5, the spectroscopic evidence is rather simple to interpret in that virtually only one component, due to the Cu–O shell, is observed. In contrast, the Ag(I)-ZSM-5 spectrum is more complicated in that, beside the main peak due to the Ag–O shell, at least two other components are observed. Quantitative data analysis was done by using experimental phases and amplitudes extracted from Cu_2O and Ag_2O model compounds (the results obtained are extensively described in [8] for Cu(I)-ZSM-5 and in refs. [21,22] for Ag(I)-ZSM-5). The following structural parameters were obtained: Cu(I) cations are surrounded by 2.5 ± 0.3 oxygen atoms at a distance of 2.00 ± 0.02 Å while Ag(I) ones are surrounded by 2.5 ± 0.5 oxygen atoms at a distance of 2.30 ± 0.03 Å. The observed differences in the metal-oxygen distance are readily assigned to the larger ionic radius of Ag(I) ($r = 1.26$ Å) as compared to the one of Cu(I) ($r = 0.96$ Å). Besides the well expected higher first shell distance, Ag(I) cations show the same coordination number (within experimental errors) found for Cu(I) cations; this indicates that Cu(I) and Ag(I) cations are located in the same kind of intrazeolite sites. The (average) value of 2.5 for the coordination numbers means that in both Cu(I)- and Ag(I)-ZSM-5 zeolites both two- and three-coordinated extra-framework cationic sites are present, in a nearly equal proportion [8,15,21,22].

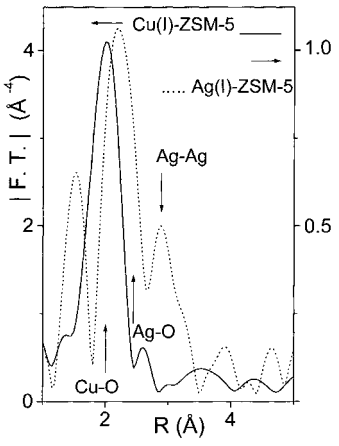

Fig. 2. The k^3-weighted (Cu–O and Ag–O) phase corrected Fourier transforms (FT) of Cu(I)-ZSM-5 (full line) and Ag(I)-ZSM-5 (dotted line). Note that, the former refers to the ordinate values reported on the left axis, while the latter refers to those reported on the right axis.

In the case of Ag-ZSM-5 sample, a component at lower distance (≈1.5 Å) has no physical meaning in that is due to unsubtracted low frequencies components in the $\chi(k)$ function obtained after estimation of the atomic absorption [21,22] whereas the peak at higher distance deserves a comment. The same peak appears in the phase uncorrected FT at the same distance (2.67 Å), where the first shell Ag–Ag is found in the Ag foil taken as model compound, but with a much lower intensity [21,22]. This means that a little amount of (at least partially) reduced silver species are present in the form of nanocluster of metallic Ag(0) or of $[Ag_n]^{x+}$ species trapped inside the MFI channels. This amount is so small (some 1% of the total Ag(I) detected) that can be reasonably neglected in discussing the results reported in this work. As for copper-exchanged ZSM-5 the amount of reduced clustered Cu(0) species, if any, are below the experimental detection limit of EXAFS spectroscopy. Thus, Cu- and Ag-ZSM-5 samples studied in the present work contain virtually only isolated Cu(I) or Ag(I) species.

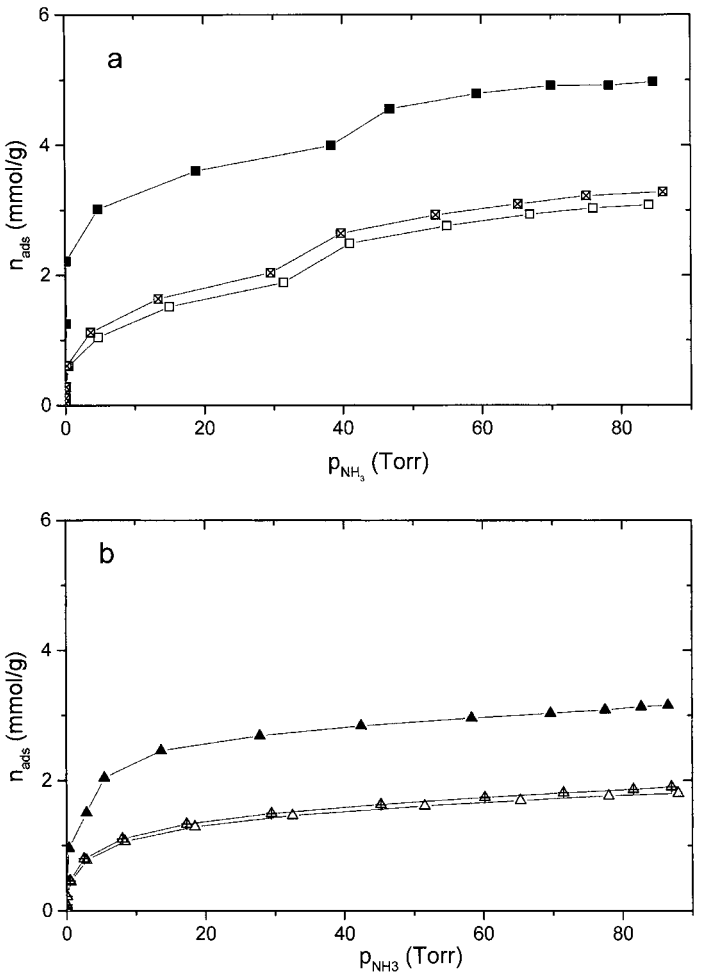

Fig. 3. (a) Volumetric isotherms (n_{ads} vs. p_{eq}) of NH_3 adsorbed at 303 K on Cu(I)-ZSM-5 activated at 673 K (solid symbol: first run; open symbols: second run; crossed symbols: third run). (b) Volumetric isotherms (n_{ads} vs. p_{eq}) of NH_3 adsorbed at 303 K on Ag(I)-ZSM-5 activated at 400 K (solid symbol: first run; open symbols: second run; crossed symbols: third run).

3.2. The formation of amino-complexes: the stoichiometry of the adducts

In Fig. 3a, the quantitative data (volumetric isotherms: first, second and third runs) of the adsorption of NH_3 on Cu(I)-ZSM-5 sample are reported. The correspondent calorimetric isotherms (integral evolved heat Q^{int} versus equilibrium p_{NH_3}) are not reported for the sake of brevity. It is clearly evident that the interaction of the probe with the activated sample is not fully reversible under the conditions adopted, in that the first and the second and third runs of adsorption (these latter performed after pumping off the sample at $p \approx 10^{-5}$ Torr for either 14 or 60 h, respectively) are not coincident. It is also evident that outgassing the sample for a longer time allows to desorb slightly larger amounts of NH_3 (the amounts adsorbed during the third run are ≈6% larger than the ones adsorbed during the second one). This result indicates that the fraction of NH_3 reversibly adsorbed at 303 K on Cu(I)-ZSM-5 depends somehow upon the time of outgassing. Thus the terms ''reversible'' and ''irreversible'' in the present case must be handled with some care. It is worth of noticing, in fact, that a couple of hours of outgassing at $p \approx 10^{-10}$ Torr allows to destroy completely the species formed in presence

of a pressure of NH_3, as witnessed by XPS data discussed in [26]. Anyway, in our experiment at $p \approx 10^{-5}$ Torr, the ammonia species are only partially desorbed from the copper-exchanged zeolite. The ''irreversible'' component measured was evaluated from the difference between first and second or third run isotherms. The amount of ammonia strongly held at the zeolite sites was found to be not dramatically different for the two different outgassing conditions examined, being some 38% of the total adsorption in the case of short outgassing and some 34% in the case of the prolonged outgassing.

In Table 1, the quantitative (adsorbed amounts per gram of zeolite and number of NH_3 molecules per Cu(I) cation) and energetic (integral heat evolved during the adsorption process per gram of zeolite and molar enthalpy of adsorption, defined as $(Q^{int}/n_{ads})_p$ at a given equilibrium pressure) data are reported for the total and the reversible adsorption of NH_3 on Cu(I)-ZSM-5. Both quantitative and energetic data are extrapolated at an equilibrium pressure of 90 Torr; this value was chosen because at this pressure the adsorption isotherms appear to approach the saturation.

In both total (first run) and reversible (second/third runs) adsorption isotherms, the shape of the curve suggests a two steps process. For the total adsorption the step in the isotherms occurs at an equilibrium pressure of ≈40 Torr, whereas for the reversible adsorption at a lower equilibrium pressure (≈30 Torr). The three runs isotherms lie parallel since the beginning of the process, indicating that the irreversible phenomena concerns only the early stages of the adsorption. The same holds for the calorimetric isotherms (not reported).

In Fig. 3b, the quantitative data (volumetric isotherms: first, second and third runs) of the adsorption of NH_3 on Ag(I)-ZSM-5 sample are reported. As in the case of Cu(I)-ZSM-5, in this one too the adsorption process is only partially reversible under the vacuum conditions adopted in the experiment ($p \approx 10^{-5}$ Torr, either 14 or 60 h), indicating that a fraction of the amino-complexes are stable upon outgassing, while the other ones are labile.

The ''irreversible'' component in this case too, corresponds to a process occurring at the very early stages of the adsorption. In both Cu(I) and Ag(I) cases, we can interpret the initial irreversible component as due to the formation of low coordination number amino adducts on the most coordinatively unsaturated Me(I) cations. Also in the Ag(I)-ZSM-5 case, the irreversible component (≈40% of the total adsorption) depends upon the time of outgassing. However, similarly to what found for Cu(I)-ZSM-5 the difference between the second and third runs isotherms is not very large (≈6%). The calorimetric isotherms (not reported) exhibit a trend similar to the volumetric ones, and it is worth of noticing that, opposite to the case of Cu(I)-ZSM-5, no steps are observed for Ag(I)-ZSM-5. The quantitative and energetic data (defined as in the case of Cu(I)-ZSM-5, see Table 1) for the total and the reversible adsorption of NH_3 on Ag(I)-ZSM-5 are reported in Table 2 and compared to the correspondent data on Cu(I)-ZSM-5.

Table 1
Quantitative (n_{ads}: adsorbed amounts per gram of zeolite; number of molecules per cation) and energetic data (Q^{int}: integral heat of adsorption per gram of zeolite; $q_p = (Q^{int}/n_{ads})_p$: molar enthalpy of adsorption at $p_{NH_3} = p$) on the adsorption of NH_3 on Cu(I)-ZSM-5 zeolite at $p_{NH_3} = 90$ Torr

	First run[a], total	Second run[b], reversible	Third run[c], reversible	First–second runs[d], irreversible	First–third runs[e], irreversible
n_{ads} (mmol/g zeolite)	4.98	3.10	3.29	1.88	1.69
NH_3 molecules/Cu(I) ion	≈5	≈3	≈3	≈2	≈2
Q^{int} (J/g zeolite)	385.3	166.6	179.3	218.7	206.0
$q_p = (Q^{int}/n_{ads})_p$ (kJ/mol)	78	54	55	116	122

[a] Total adsorption.
[b] Reversible adsorption (after short outgassing).
[c] Reversible adsorption (after prolonged outgassing).
[d] Irreversible adsorption (after short outgassing).
[e] Irreversible adsorption (after prolonged outgassing).

Table 2
Quantitative (n_{ads}: adsorbed amounts per gram of zeolite; number of molecules per cation) and energetic data (Q^{int}: integral heat of adsorption per gram of zeolite; $q_p = (Q^{int}/n_{ads})_p$: molar enthalpy of adsorption at $p_{NH_3} = p$) on the adsorption of NH_3 on Ag(I)-ZSM-5 zeolite at $p_{NH_3} = 90$ Torr

	First run[a] total	Second run[b] reversible	Third run[c] reversible	First–second runs[d] irreversible	First–third runs[e] irreversible
n_{ads} (mmol/g zeolite)	3.18	1.80	1.92	1.38	1.26
NH_3 molecules/Cu(I) ion	≈3	≈2	≈2	≈1	≈1
Q^{int} (J/g zeolite)	249.4	93.7	100.8	155.7	148.6
$q_p = (Q^{int}/n_{ads})_p$ (kJ/mol)	78	52	53	113	118

[a] Total adsorption.
[b] Reversible adsorption (after short outgassing).
[c] Reversible adsorption (after prolonged outgassing).
[d] Irreversible adsorption (after short outgassing).
[e] Irreversible adsorption (after prolonged outgassing).

The amounts of NH_3 adsorbed (mmol/g zeolite) on Cu(I)-ZSM-5 are much higher than the amounts adsorbed on Ag(I)-zeolite, at any equilibrium pressure examined. However, the interaction of NH_3 with sites other than the noble Me(I) cations should be the same in the two cases: indeed the zeolite matrix is the same, and all the protons in the H-ZSM-5 precursor have been totally exchanged by Cu(I) or Ag(I) cations (vide supra, Fig. 1). Thus, the significant different amounts of ammonia adsorbed on the two systems imply that Cu(I) and Ag(I) cations bind a different number of ligands. In order to quantify the number of amino ligands surrounding Cu(I) cations, the amounts adsorbed per gram of zeolite were transformed into a number of NH_3 molecules adsorbed per metal cation (see Tables 1 and 2). In particular, the number of NH_3 molecules per cation (at $p_{NH_3} = 90$ Torr) is ≈5 in the case of Cu(I) sites and ≈3 for the Ag(I) ones. As for the reversible adsorption (second/third runs) the number of NH_3 molecules is ≈3 for Cu(I) and ≈2 for Ag(I) cations. These data suggest that in the case of Cu(I) the tetra-amino complexes $[Cu(NH_3)_4]^+$ are formed and beside to the NH_3 molecules acting as ligands to Cu(I), an additional amount of ammonia interacts with the zeolite matrix, most likely via H-bond with the residual external SiOH groups (vide supra, Fig. 1). At $p_{NH_3} = 40$ Torr (at which the first run isotherms exhibit a step), the tetra-amino-adducts are already formed, as witnessed by the fact that the number of NH_3 molecules per Cu(I) cation are close to four. The amounts adsorbed after this step up to the saturation plateau corresponds roughly to one NH_3 molecule per cation. The average molar enthalpy of adsorption at $p_{NH_3} = 90$ Torr is $q_{90} = (Q^{int}/n_{ads})_{90} \approx 78$ kJ/mol.

In the case of Ag(I)-ZSM-5, for which no steps are observed in the isotherms, the total adsorbed amounts is close to three molecules of NH_3 per Ag(I) cation. This figure can be interpreted as due to the formation of di-amino $[Ag(NH_3)_2]^+$ species accompanied by the adsorption of an additional amount of ammonia weakly bound to the zeolite SiOH groups (see the case of Cu(I)-ZSM-5). The average molar enthalpy of adsorption is $q_{90} = (Q^{int}/n_{ads})_{90} \approx 78$ kJ/mol. Notice that, in spite of the different stoichiometry of the amino adducts the two Me(I) cations form, their average heat of formation is very close.

The present results, concerning the Lewis acid–base interaction in intrinsically heterogeneous systems, are in good agreement with the homogeneous chemistry data of copper and silver cations. Indeed, the favourite coordination number of Cu(I) in solution is 4, implying a tetrahedral geometry, whereas is 2 for Ag(I), implying a linear geometry [23]. In the present heterogeneous systems, in addition, the different size of the two cations, and consequently the different steric hindrance in the zeolite cavities, likely play a role in depressing the number of ligands the large Ag(I) cations are able to bind with respect to the much smaller Cu(I) ones.

In the case of Cu(I), the number of molecules reversibly adsorbed per metal cation is close to three. This means that, beside the ammonia weakly and intrinsically reversibly adsorbed on the zeolite SiOH groups (corresponding to one NH_3 molecule/cation), two of

the four molecules participating to the formation of the adducts $[Cu(NH_3)_4]^+$ are bound more weakly than the other two, and do not resist to the pumping off. The average molar enthalpy of the reversible adsorption on Cu(I) sites is $q_{90} = (Q^{int}/n_{ads})_{90} \approx$ 54–55 kJ/mol, the former value corresponding to the second run and the latter to the third one. In the case of Ag(I) too, one half of the $[Ag(NH_3)_2]^+$ adducts are destroyed by pumping off at RT The number of molecules reversibly adsorbed is ≈2 per Ag(I) cation, but a fraction of this amount corresponds to the weakly bound ammonia interacting with the zeolite silanols. The average molar enthalpy of the reversible adsorption on Ag(I) is $q_{90} \approx$ 52–53 kJ/mol, slightly lower than the one measured for Cu(I) system.

3.3. Energetics of the amino-complexes formation

In order to better describe the energetics of the interaction of NH_3 with the metal cations, the differential heats of adsorption (first, second and third runs) of NH_3 on Cu(I)-ZSM-5 are reported as a function of the adsorbed amounts, as shown in Fig. 4a.

The enthalpy of adsorption strongly depends upon surface coverage, in that the heat values decrease from an initial very high q_0 (enthalpy of adsorption extrapolated to vanishing coverage) of ≈180 kJ/mol for the first run; ≈100 and 120 kJ/mol for the second and the third one, respectively) down to ≈30–40 kJ/mol. In the inset of the figure the integral heats of adsorption versus the adsorbed amounts plot (first run only) is reported as a polynomial of order 3 (see figures caption for the best fit parameters). The very high q_0 obtained for the first run are ascribed to the fact that at the very early stages of the adsorption a little amount (<2% of the total ammonia adsorbed) of sites, able to interact quite strongly and irreversibly with NH_3, are present on the Cu(I)-ZSM-5 system. The nature of such highly energetic sites was tentatively interpreted on the basis of XPS evidence [26] as due to the interaction of ammonia with sites of defective nature, likely trigonal Al(III) atoms. The fact that in the case of the third run adsorption (performed after a prolonged outgassing at 303 K) the q_0 value is higher than the one obtained for the second run is ascribable to fact that the pumping off in more severe conditions (60 h instead of 14 h) allows an additional little amount of the more highly energetic amino-complexes to be destroyed. However, as indicated by the almost complete absence of the 130–100 kJ/mol region in both second and third runs curves, the large majority of the more energetic adducts are stable upon outgassing and are not destroyed by pumping off at $p \approx 10^{-5}$ Torr, either only 14 or even 60 h.

On the basis of the shape of the curve, it is possible to distinguish three different domains in the first run of adsorption curve, and two in the second and third runs as far as the coverage increases: (i) a highly energetic ($130\,kJ/mol < q_{ads} < 100\,kJ/mol$) and irreversible (in the adopted conditions) interaction; (ii) a less energetic ($100\,kJ/mol < q_{ads} < 50\,kJ/mol$) and reversible interaction; (iii) a low energetic and reversible interaction ($q_{ads} < 50$ kJ/mol), at the highest coverage attained (correspondent to the saturation of the isotherm). This low energetic interaction is likely due to the adsorption of NH_3 on SiOH groups which presence in the zeolite matrix is indicated by the IR spectra shown in Fig. 1 (vide supra). These sites are capable of interacting with NH_3 via H-bonding (with a heat of adsorption of 30–40 kJ/mol) as discussed in detail in the case of silicalite systems [31]. The more energetic values (both irreversible and reversible in nature) are assumed to be specific of the interaction with cus Cu(I) cations, able to form amino-complexes of different stability. By shifting the second/third runs curves of ≈1.8 mmol/g (equivalent to ≈2 molecules/Cu(I) cation) the curves are virtually overlapped, within the experimental error, to the first run curve. The irreversible component of the process thus roughly corresponds to the adsorption of ≈2 molecules/Cu(I) cation. This datum confirms that two of the four ligands of the tetra-amino $[Cu(NH_3)_4]^+$ complexes are more stable than the other two.

In Fig. 4(b), the evolution of the heat of adsorption with NH_3 coverage is reported for the Ag(I)-ZSM-5 system. In the inset of the figure the integral heats of adsorption versus the adsorbed amounts plot (first run only) is reported as a polynomial of order 3, as in the case of Cu(I)-ZSM-5. Similarly to what observed for Cu(I)-ZSM-5, apart from a very few sites interacting with ammonia with a quite high heat of adsorption ($q_0 \approx 180$ kJ/mol), three regions characterised by the heat values quite close to the ones measured for Cu(I)-ZSM-5 can be observed in the heat versus coverage plot. Both irreversible and reversible adsorption of

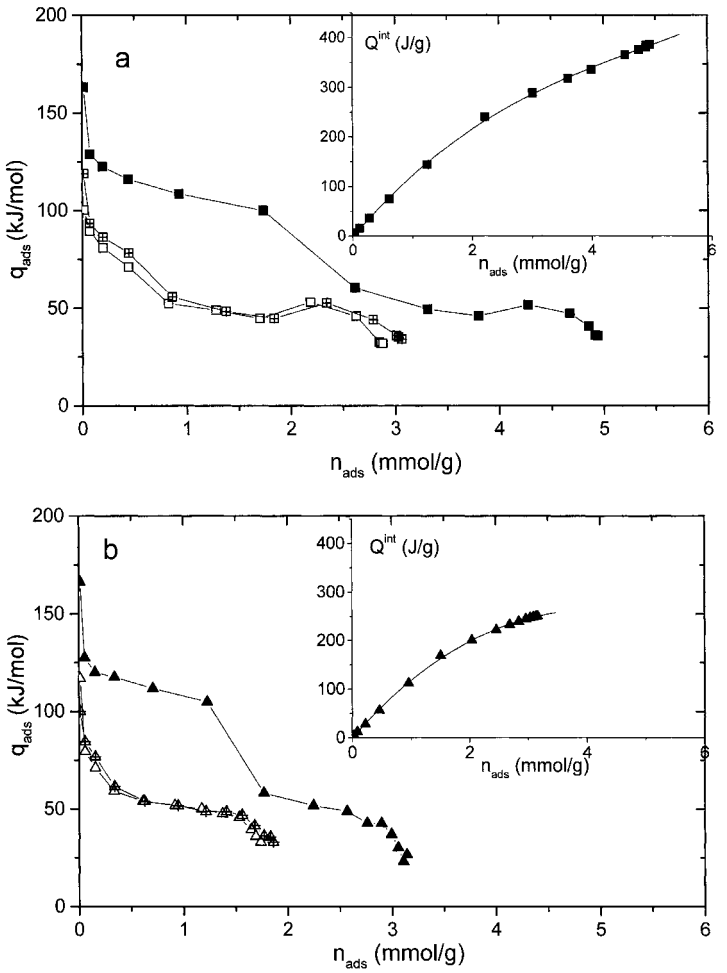

Fig. 4. (a) Differential heats of adsorption (q_{ads}) of NH_3 on Cu(I)-ZSM-5 activated at 673 K (solid symbol: first run; open symbols: second run; crossed symbols: third run) as a function of the adsorbed amounts (n_{ads}). Inset: integral heats of adsorption (Q^{int}) as a function of adsorbed amounts (n_{ads}), first run. The interpolated line has been obtained by a polynomial regression: $Q^{int} = a + b_1 n_{ads} + b_2 n_{ads}^2 + b_3 n_{ads}^3$ ($a = -0.89541 \pm 1.66467$; $b_1 = 140.13165 \pm 6.09816$; $b_2 = -22.03832 \pm 4.63192$; $b_3 = 0.90502 \pm 0.93692$). (b) Differential heats of adsorption (q_{ads}) of NH_3 on Ag(I)-ZSM-5 activated at 400 K (solid symbol: first run; open symbols: second run; crossed symbols: third run) as a function of the adsorbed amounts (n_{ads}). Inset: integral heats of adsorption (Q^{int}) as a function of adsorbed amounts (n_{ads}), first run. The interpolated line has been obtained by a polynomial regression: $Q^{int} = a + b_1 n_{ads} + b_2 n_{ads}^2 + b_3 n_{ads}^3$ ($a = -1.60239 \pm 2.55879$; $b_1 = 142.33964 \pm 6.23589$; $b_2 = -19.27928 \pm 3.02351$; $b_3 = 1.2605 \pm 0.38618$).

NH_3 with a heat higher than 50 kJ/mol are assigned to a specific interaction of the probe with the cus Ag(I) cations, giving rise to amino complexes. The so formed adducts are either stable or labile upon outgassing at 303 K ($p \approx 10^{-5}$ Torr), but in both cases they do form with a heat very close to the one measured for Cu(I)-ZSM-5. This datum suggests that the amino ligands do not discriminate the two noble Me(I) cations from an energetic point of view.

Again, if the second/third runs curves are shifted of ≈1.2 mmol/g, the first and the second/third runs curves overlap each other within the experimental error. This amount corresponds to the irreversible component, indicating that ≈1 molecule per cation is strongly held on Ag(I) sites with a heat of adsorption higher than 100 kJ/mol. The low energetic region ($q < 50$ kJ/mol) corresponds also in the Ag(I)-ZSM-5 case to a H-bonding interaction of NH_3 with SiOH

groups present in the external surface of the zeolite matrix. The number of NH_3 molecules weakly adsorbed ($q < 50$ kJ/mol) reported per metal cation is larger in the case of Ag(I) with respect to the case of Cu(I). This datum can be interpreted by taking into account that at a same equilibrium pressure of ammonia, the stoichiometry of the amino-complexes corresponds to a number of coordination lower in the case of Ag(I) than in the case of Cu(I). Being lower the number of molecules of NH_3 forming the adducts, the amount of physisorbed molecules increases. The final value of the heat of adsorption of NH_3 is quite low in the case of Ag(I), being ≈25 kJ/mol, approaching the heat of liquefaction of NH_3. The narrowness of the zeolite cavities favours indeed the liquid-like physisorption of NH_3 [31].

3.4. IR spectroscopy of the amino-complexes

The non complete reversibility upon outgassing at ≈300 K of the tetra-amino $[Cu(NH_3)_4]^+$ and di-amino $[Ag(NH_3)_2]^+$ complexes formed at the cationic sites in the zeolite structure was revealed also by IR spectroscopy. In fact, prolonged outgassing at RT up to a final vacuum of 10^{-4} Torr implies a reduction of some 60% of the intensities of the bands ascribed to NH_3: the δ(NH) one at 1610 cm^{-1} and the ν(NH) in the 3500–3100 cm^{-1} interval (not reported for the sake of brevity: see [24]). This datum is in good agreement with the reversible amount of ammonia determined by volumetric-calorimetric experiments. No evidence of formation NH_4^+ cations was detected, confirming once again that we are dealing with a virtually 200% exchanged sample where virtually all protons in H-ZSM-5 zeolite have been replaced by Cu(I) or Ag(I) cations.

3.5. The formation of mixed amino-carbonyl complexes

In Fig. 5, the quantitative and energetic data of the adsorption of CO on Cu(I)-ZSM-5 zeolite previously contacted with NH_3 (up to $p_{NH_3} \approx 90$ Torr) and subsequently outgassed at 303 K are reported. In this case, Cu(I) sites are not coordinatively unsaturated as in the virgin Cu(I)-ZSM-5, but are already engaged in the stable amino $[Cu(NH_3)_n]^+$ adducts (with $2 \leq n \leq 1$) not destroyed by the RT outgassing. In Fig. 5(a), volumetric isotherms (first and second runs, circle symbols, bottom side curves) are shown. The isotherms obtained for the total (first run) adsorption of NH_3 on the bare Cu(I)-ZSM-5 systems are reported (square symbols, top side curves) for comparison. The amounts of CO adsorbed on the sample containing the $[Cu(NH_3)_n]^+$ adducts in the zeolite cavities are dramatically lower than the amounts adsorbed on the bare cus Cu(I) cations. It is worth of noticing that in the case of the sample previously contacted with NH_3 the second run of the adsorption of CO curve is surprisingly higher than the first one. This datum suggests that the presence of CO as additional ligand on Cu(I) sites allows a slightly larger amount of amino-complexes to be destroyed upon outgassing. The same trend is shown by the calorimetric isotherms (not reported). In Fig. 5(b), the heat of adsorption versus coverage plots for the two cases (i.e. CO adsorbed on Cu(I)-ZSM-5 and on $[Cu(NH_3)_n]^+$ entrapped in the zeolite cavities) are reported. The presence of stable amino-complexes in the zeolite cavities dramatically decreases not only the amount of the carbonyl-like species formed with respect to the virgin outgassed Cu(I)-ZSM-5 sample, but also their heat of formation. Indeed the q_0 for the CO adsorbed on the sample containing the amino-complexes is only ≈80 kJ/mol, whereas for the bare cus Cu(I) cations is ≈120 kJ/mol. Further, in the former case the heat of adsorption versus coverage curves range in the 80–45 kJ/mol interval, whereas in the latter in the 120–60 kJ/mol interval. Indeed, being all Cu(I) cations engaged with at least one NH_3 molecule forming mono-amino-complexes, or with more than one NH_3 ligands forming poly-amino-complexes (vide supra: the stoichiometry of the adducts), the best CO molecules can do is to be inserted in the mono-amino-complexes forming the mixed amino-carbonyl complexes (as witnessed by the IR spectra, vide infra). The presence of charge-releasing NH_3 species on the Cu(I) sites significantly decrease the actual charge of the cations and then their energy of interaction with CO (i.e. their Lewis acidity). At $p_{CO} = 20$ Torr, the difference between the amounts of CO adsorbed on the virgin outgassed sample and the sample pre-contacted by NH_3 are 1,19 mmol/g, corresponding to ≈1 CO molecule/Cu(I) cation. The population of sites available for CO in presence of $[Cu(NH_3)_n]^+$ complexes is

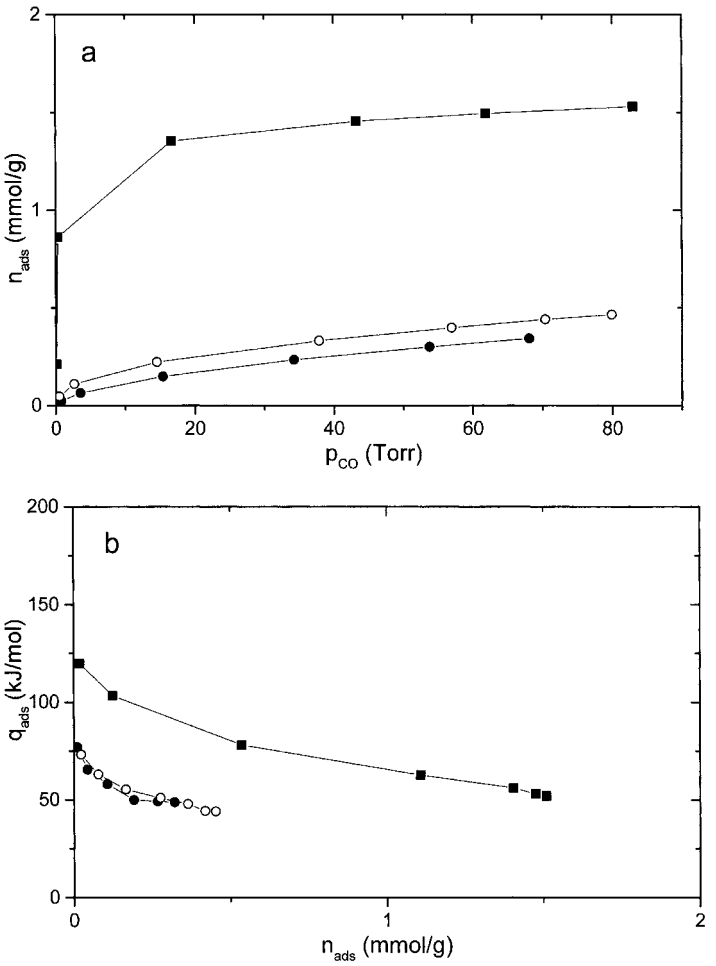

Fig. 5. (a) Volumetric isotherms (n_{ads} vs. p_{eq}) of CO adsorbed at 303 K on Cu(I)-ZSM-5 activated at 673 K, contacted with NH_3 ($p_{NH_3} \approx 90$ Torr) and subsequently outgassed at 303 K in order to eliminate only the irreversible component of the copper amino-complexes (circle; solid symbols: first run; open symbols: second run of adsorption). The volumetric isotherm (first run) of CO adsorbed on the bare Cu(I)-ZSM-5 sample (square; solid symbols) is reported for comparison. (b) Differential heats of adsorption (q_{ads}) of CO on the samples described in part (a), as a function of the adsorbed amounts (n_{ads}). Symbols as in (a).

decreased of 80% of the total sites available at $p_{CO} = 90$ Torr.

In Fig. 6, the quantitative and energetic data of the adsorption of NH_3 on Cu(I)-ZSM-5 zeolite previously contacted with CO (up to $p_{CO} \approx 90$ Torr) and subsequently outgassed at 303 K are reported. In these conditions a fraction of mono-carbonyl $[Cu(CO)]^+$ adducts stable upon outgassing are still present in the zeolite pores. In Fig. 6(a), the volumetric isotherms are shown. The curves obtained for the total (first run) adsorption of NH_3 on the bare Cu(I)-ZSM-5 systems are also reported (square symbols, top side curve) for comparison. The shape of the volumetric isotherms of the NH_3 adsorbed on the sample containing the previously formed monocarbonyl complexes (circle symbols, bottom side curve) is significantly different from that obtained for NH_3 adsorbed on the bare cus Cu(I) cations, and mostly at the beginning of the process ($p_{NH_3} < 20$ Torr). At higher NH_3 equilibrium pressure, the two isotherms tend to merge; notice that a step is observed in the curve also in this case, but shifted to higher values with respect to the case of the

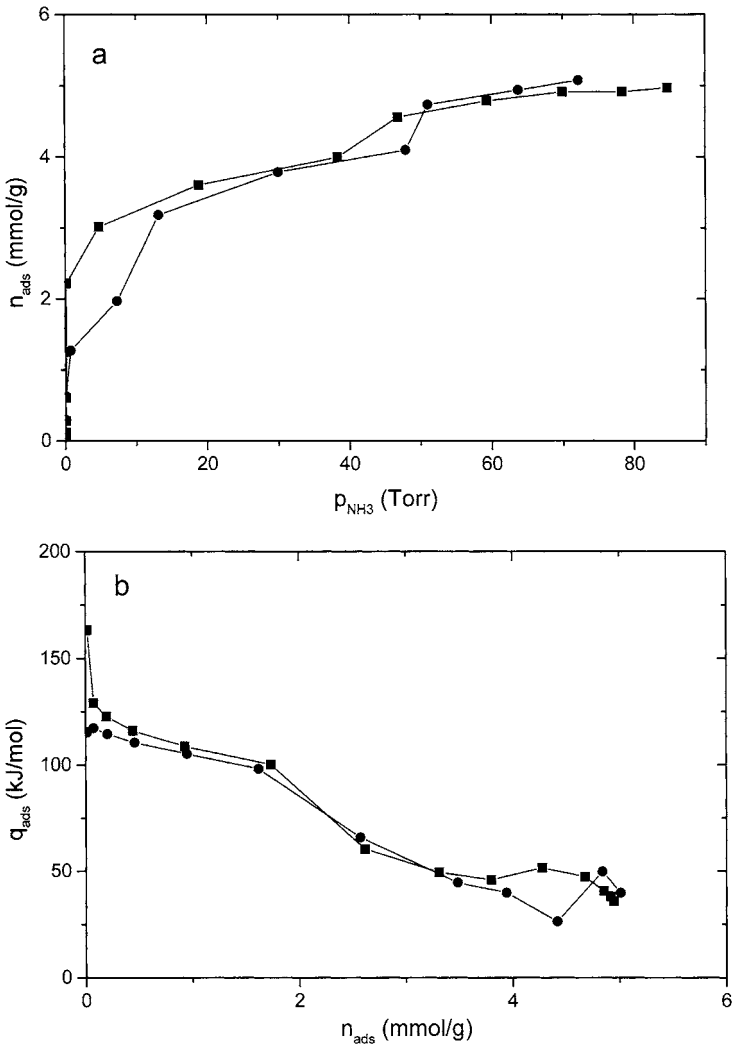

Fig. 6. (a) Volumetric isotherms (n_{ads} vs. p_{eq}) of NH_3 adsorbed at 303 K on Cu(I)-ZSM-5 activated at 673 K, contacted with CO ($p_{CO} \approx 90$ Torr) and subsequently outgassed at 303 K in order to eliminate only the irreversible component of the copper carbonil-like species (circle, solid symbols, first run). The volumetric isotherm (first run) of NH_3 adsorbed on the bare Cu(I)-ZSM-5 sample (square, solid symbols) is reported for comparison (see Fig. 3a). (b) Differential heats of adsorption (q_{ads}) of NH_3 on the samples described in (a), as a function of the adsorbed amounts (n_{ads}).

cus Cu(I) cations (≈50 instead of ≈40 Torr). As for the calorimetric isotherms (not reported) the curve correspondent to the adsorption of NH_3 on the Cu(I) cations already engaged with CO lies lower of the reference isotherm, in the whole equilibrium pressure interval examined. This datum suggests that the amount of heat evolved during the whole process is lower than in the case of the adsorption of NH_3 on the bare cus Cu(I) cations. This suggestion is confirmed by the heat of adsorption versus coverage plot reported in Fig. 6(b). In the case of the adsorption of NH_3 on the sample previously contacted with CO, the most energetic sites observed in the case of the virgin sample are virtually totally absent. This means that these sites are already occupied by the most strongly held mono-carbonyl-species, but as far as the NH_3 equilibrium pressure increases (and consequently the coverage increases) the NH_3 molecules

adsorb on both the cus Cu(I) and $[Cu(CO)]^+$ sites forming both amino- and mixed amino-carbonyl complexes. The total amount of NH_3 adsorbed at $p_{NH_3} \approx 90$ Torr is virtually the same as in the case of the outgassed sample (see Fig. 3a and Table 1).

3.6. Infrared spectroscopy of mixed amino-carbonyl complexes

In Fig. 7, the room temperature IR spectra of CO adsorbed on the sample containing $[Cu(NH_3)_n]^+$ species in the zeolite cavities (section (a)) and the IR spectra of NH_3 adsorbed on the sample containing the mono-carbonyl $[Cu(CO)]^+$ species (section (b)) are shown. The two cases appear definitely different to each other. In Fig. 7(a), it is possible to note the progressive increase of the intensity of the band at increasing doses of CO (up to ≈20 Torr) on the sample containing $[Cu(NH_3)_n]^+$ species. The presence of CO as additional ligand does not perturb at all the spectral features of the preadsorbed NH_3: in the inset of the figure the bending mode δ(NH) located at 1616 cm^{-1} is shown for the case of NH_3 bound to Cu(I) sites (curve 1) and in presence of the increasing doses of CO (curves 2–10). While the CO stretching band increases in intensity as far as the p_{CO} pressure increases, the 1616 cm^{-1} band does not change in intensity and remains at the same spectral position. However, it is worth noticing that the spectral position of CO adsorbed is significant lower ($\nu_{CO} = 2100$ cm^{-1}) with respect to the one observed for CO adsorbed on the bare cus Cu(I) cations ($\nu_{CO} =$ 2157 cm^{-1}). The downward shift ($\Delta\nu \approx -60$ cm^{-1}) of the ν(CO) band observed with respect to the monocarbonylic species in absence of NH_3 indicates that the presence of NH_3 as additional ligand does increase the electron density of the Lewis acidic Cu(I) cations, confirming the calorimetric results giving a heat of adsorption values ranging in a lower values interval with respect to the bare Cu(I)-ZSM-5 system (vide supra).

In Fig. 7b, the opposite situation is described: the intensity of the 2157 cm^{-1} band, characteristic of CO adsorbed on cus Cu(I) cations, decreases (curves 1–5) as far as increasing amounts of NH_3 are adsorbed on the sample. The increasing amounts of NH_3 adsorbed

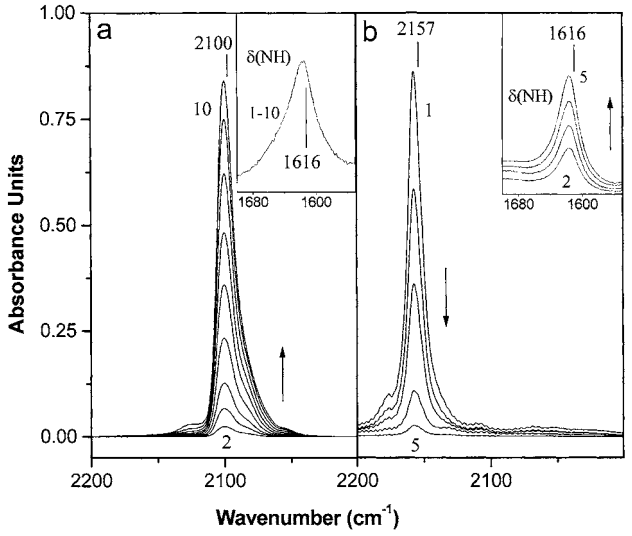

Fig. 7. (a) IR spectra of CO adsorbed (≈300 K; curves 2–10 refer to increasing CO pressure up to ≈20 Torr) on Cu(I)-ZSM-5 activated at 673 K, pre-contacted with NH_3 ($p_{NH_3} \approx 90$ Torr) and subsequently outgassed at 303 K in order to eliminate only the irreversible component of the copper amino-complexes. In the inset: the δ(NH) bending mode of NH_3 bound to Cu(I) sites is reported, at increasing p_{CO} (curves 1–10). (b) IR spectra of NH_3 adsorbed (≈300 K; curves 1–5 refer to increasing NH_3 pressure up to ≈20 Torr) on Cu(I)-ZSM-5 activated at 673 K, pre-contacted with CO ($p_{CO} \approx 90$ Torr) and subsequently outgassed at 303 K in order to eliminate only the irreversible component of the carbonyl-like species. In the inset: the δ(NH) bending mode of NH_3 progressively bound to Cu(I) sites is reported at increasing p_{NH_3} (curves 2–5).

are monitored by the increasing intensity of the bending mode δ(NH) located at 1616 cm^{-1}, as shown in the inset of the figure (curves 2–5).

In both cases examined, there is a clear spectroscopic evidence that mixed carbonyl-amino complexes can form at the Cu(I) sites in the ZSM-5 zeolite. However, a different stability of the amino $[Cu(NH_3)_n]^+$ and the carbonyl $[Cu(CO)]^+$ adducts was observed, as already suggested by the volumetric–calorimetric data. In particular, while NH_3 molecules causes the previously bound CO ligands to be eventually eliminated by the Cu(I) sites, CO molecules are not able to do the same with the previously bound amino ligands.

4. Conclusions

The RT adsorption of NH_3 was used to investigate the coordinative unsaturation of Cu(I) and Ag(I) cations located in the ZSM-5 channels sites. The investigation, carried out by the combined use of IR spectroscopy and microcalorimetry, allowed the nature, stability upon outgassing, stoichiometry and heat of formation of the adducts formed at the metal cation sites to be described in details. Cu(I) cations do form tetra-amino species, stable upon an equilibrium pressure of NH_3 higher than 40 Torr, whereas the coordination number of the analogous Ag(I) complexes was found to be lower. Indeed Ag(I) sites do form only diamino species stable in the same conditions as for Cu(I). The coordination number of 4 and 2 is in good agreement with the coordination homogeneous chemistry of these species. The adducts formed are only partially labile upon outgassing ($p \approx 10^{-5}$ Torr) at RT, confirming the ability of the zeolite framework to have a ''protective effect'' on the entrapped species. The heat of formation of amino species was found to be very close for Cu(I) and Ag(I) sites, in spite of their different stoichiometry. The formation of mixed amino-carbonyl species at the Cu(I) sites have been studied: the behavior of CO and NH_3 ligands was found to be not the same. In particular, CO ligands can be inserted in the previously formed $[Cu(NH_3)_n]^+$ adducts, whereas NH_3 ones are able to displace CO from the previously formed $[Cu(CO)]^+$ species. The thermodynamical stability of the amino- and carbonyl-complexes is thus different, in spite of the enthalpy of formation quite close for the two kinds of adducts and comprised in the 130–50 kJ/mol interval, according to the number of ligands bound to the Me(I) cations. EXAFS spectroscopy was used to check the local environment of the metal cations: the atomic resolution data and the molar quantitative and energetic data were found to be in a quite good agreement.

Acknowledgements

The present work is part of a research project coordinated by Prof. A. Zecchina and cofinanced by the Italian MURST (Cofin 98, Area 03). One of us (Gemma Turnes Palomino) is grateful to the European Community for a TMR grant. X-ray absorption measurements have been performed at the BM8 GILDA beamline at the ESRF within the public user program. The authors are also indebted with all the GILDA technical staff (in particular with F. Danca and F.D'Acapito) and with ESRF Chem. Lab. (in particular with Dr. Müller), who have allowed us to work under optimal conditions. The GILDA beamline is financed by INFM, INFN, CNR.

References

[1] M. Iwamoto, H. Hamada, Catal. Today 10 (1991) 57.
[2] Y. Li, W.K. Hall, J. Phys. Chem. 94 (1990) 6145.
[3] M. Shelef, Chem. Rev. 95 (1995) 209 and references therein.
[4] T. Sun, K. Seff, Chem. Rev. 94 (1994) 857 and references therein.
[5] P.A. Jacobs, J.B. Uytterhoeven, H.K. Beyer, J. Chem. Soc., Chem. Commun. (1977) 128.
[6] G. Calzaferri, S. Hug, T. Hugentobler, B. Sulzberger, J. Photochem. 26 (1984) 109.
[7] G.D. Borgard, S. Molvik, P. Balaram, T.W. Root, J.A. Dumesic, Langmuir 11 (1995) 2065.
[8] C. Lamberti, S. Bordiga, M. Salvalaggio, G. Spoto, A. Zecchina, F. Geobaldo, G. Vlaic, M. Bellatreccia, J. Phys. Chem. B 101 (1997) 344 and references therein.
[9] A. Zecchina, S. Bordiga, M. Salvalaggio, G. Spoto, D. Scarano, C. Lamberti, J. Catal. 173 (1998) 500.
[10] D. Lai, J. Li, P. Huang, D. Wang, J. Mater. Gas. Chem. 3 (1994) 211.
[11] Y. Inoue, K. Nakashiro, Y. Ono, Micropor. Mater. 4 (1995) 379.
[12] K.I. Hadjiivanov, Micropor. Mesopor. Mater. 24 (1998) 41.
[13] A. Ozin, A. Kuperman, A. Stein, Angew, Chem. Int. Ed. Engl. 28 (1989) 359.
[14] T. Bein, P. Enzel, Angew. Chem. Int. Ed. Engl. 28 (1989) 1692.

[15] A. Zecchina, S. Bordiga, G. Turnes Palomino, D. Scarano, C. Lamberti, M. Salvalaggio, J. Phys. Chem. B 103 (1999) 3833.
[16] P.K. Hurlburt, J.J. Rack, S.F. Dec, O.P. Anderson, S.H. Strauss, Inorg. Chem. 32 (1993) 373.
[17] K. Hurlburt, H. Willner, F. Aubke, Angew. Chem. Int. Ed. Engl. 36 (1997) 2403.
[18] G. Spoto, S. Bordiga, G. Ricchiardi, D. Scarano, A. Zecchina, F. Geobaldo, J. Chem. Soc., Faraday Trans. 91 (1995) 3285.
[19] G. Spoto, A. Zecchina, S. Bordiga, G. Ricchiardi, G. Martra, G. Leofanti, G. Petrini, Appl. Catal. B 3 (1994) 151.
[20] C. Lamberti, G. Turnes Palomino, S. Bordiga, G. Berlier, F. D'Acapito, A. Zecchina, Angew. Chem. Int. Ed. Engl. 39 (2000) 2138.
[21] S. Bordiga, C. Lamberti, G. Turnes Palomino, F. Geobaldo, D. Arduino, A. Zecchina, Micropor. Mesopor. Mater. 30 (1999) 129.
[22] S. Bordiga, G. Turnes Palomino, D. Arduino, C. Lamberti, A. Zecchina, C. Otero Areán, J. Mol. Catal. A 146 (1999) 97.
[23] N.N. Greenwood, A. Earnshaw, in: The Chemistry of the Elements, Butterworths, London, 1984, p. 1386.
[24] V. Bolis, S. Bordiga, C. Lamberti, V. Graneris, G. Turnes Palomino, A. Zecchina, Stud. Surf. Sci. Catal. 130 (2000) 3261.
[25] W. Grunert, N.W. Hayes, R.W. Joyner, E.S. Shpiro, M. Rafiq, H. Siddiqui, G.N. Baeva, J. Phys. Chem. 98 (1994) 10832.
[26] V. Bolis, S. Maggiorini, L. Meda, S. Bordiga, G. Turnes Palomino, F. D'Acapito, C. Lamberti, J. Chem. Phys. 113 (2000) 9248.
[27] V. Bolis, S. Bordiga, C. Lamberti, A. Zecchina, A. Carati, G. Petrini, F. Rivetti, G. Spanò, Micropor. Mesopor. Mater. 30 (1999) 67.
[28] V. Bolis, S. Bordiga, C. Lamberti, A. Zecchina, A. Carati, G. Petrini, F. Rivetti, G. Spanò, Langmuir 15 (1999) 5753.
[29] F.W. Lytle, D.E. Sayers, E.A. Stern, Physica B 158 (1989) 701.
[30] A. Michalowicz, J. Phys. IV (France) 7 (1997) C2–235.
[31] S. Bordiga, I. Roggiero, P. Ugliengo, A. Zecchina, V. Bolis, G. Artioli, C. Lamberti, J. Chem. Soc., Dalton Trans. (2000) 3921.